Ionization and Phase Behavior of Fatty Acids in Water: Application of the Gibbs Phase Rule†

David P. Cistola,* James A. Hamilton, David Jackson, and Donald M. Small

Biophysics Institute, Housman Medical Research Center, Departments of Medicine and Biochemistry, Boston University School of Medicine, Boston, Massachusetts 02118

Received August 11, 1987; Revised Manuscript Received November 17, 1987

ABSTRACT: The phase behavior of several medium-chain (10- and 12-carbon) and long-chain (18-carbon) fatty acids in water was examined as a function of the ionization state of the carboxyl group. Equilibrium titration curves were generated above and below fatty acid and acid–soap chain melting temperatures and critical micelle concentrations, and the phases formed were characterized by X-ray diffraction, ^{13}C NMR spectroscopy, and phase-contrast and polarized light microscopy. The resulting titration curves were divided into five regions: (i) at pH values <7, a two-phase region containing oil or fatty acid crystals and an aqueous phase; (ii) at pH ~7, a three-phase region containing oil, lamellar, and aqueous (or fatty acid crystals, 1:1 acid–soap crystals, and aqueous) phases; (iii) between pH 7 and 9, a two-phase region containing a lamellar fatty acid/soap (or crystalline 1:1 acid–soap) phase in an aqueous phase; (iv) at pH ~9, a three-phase region containing lamellar fatty acid–soap (or crystalline 1:1 acid–soap), micellar, and aqueous phases; and (v) at pH values >9, a two-phase region containing micellar and aqueous phases. Interpretation of the results using the Gibbs phase rule indicated that, for oleic acid/potassium oleate, the composition of the lamellar fatty acid/soap phase varied from ~1:1 to 1:3 un-ionized to ionized fatty acid species. In addition, constant pH regions observed in titration curves were a result of thermodynamic invariance (zero degrees of freedom) rather than buffering capacity. The results provide insights into the physical states of fatty acids in biological systems. The predominant phase formed at physiologic pH and temperature is the lamellar fatty acid/soap phase. In addition, fatty acids in water do not form a micellar phase below pH 9, and hence, it is unlikely that local accumulations of nonesterified fatty acids could exert detergent effects on cellular membranes, as has been widely suggested.

It is well-known that the physical properties of "fatty acids"[1] in water are influenced by the ionization state of the carboxyl group (Small, 1986). We recently examined the phase behavior of fatty acids (1:1 acid–soaps) in water at half-ionization as a function of water content and temperature using X-ray diffraction, differential scanning calorimetry, and polarized light microscopy (Cistola et al., 1986). The results indicated that medium- and long-chain "fatty acids" in water at half-ionization spontaneously form crystalline and liquid-crystalline aggregates (e.g., inverted hexagonal and bilayer structures), but not micelles.

In the present study, we examined the phase behavior of medium- and long-chain "fatty acids" in water as a function of the ionization state of the carboxyl group. The objectives of this study were 4-fold: (i) to systematically determine titration curve profiles and "fatty acid" physical states formed above and below fatty acid and acid–soap chain melting temperatures, above and below fatty acid solubility limits, and above and below critical micelle concentration (cmc)[2] values; (ii) to examine each phase formed using physicochemical techniques (X-ray diffraction, ^{13}C NMR spectroscopy, and phase-contrast and polarized light microscopy); (iii) to prepare samples in such a way as to ensure that equilibrium was reached so that the Gibbs phase rule could be applied; and (iv) to demonstrate the usefulness of the phase rule in predicting the shape of titration curves and the number of phases formed by "fatty acids" in water. The results provide insights into the physical states formed by localized accumulations of "fatty acids" at different ionization states in vivo.

Materials and Methods

Potassium decanoate, laurate, and oleate were purchased from Nu Chek Prep (Elysian, MN) and used without further purification. Sample purity was >99%, as analyzed by thin-layer and gas–liquid chromatography. HCl solutions (0.94 M) were standardized against potassium acid phthalate using phenophthalein and pH measurements as end-point indicators.

For initial titrations of fatty acids above their monomer solubility limit, aggregation and/or phase separation occurred, and samples required a long time to reach equilibrium. Therefore, the following procedures were used to ensure that equilibrium was reached. A 100-mL solution of 0.08 M potassium decanoate or oleate or 0.21 M potassium laurate was prepared, and 2.5 mL of this solution was pipetted into each of 40 clean glass scintillation vials. An appropriate amount of titrant (0.94 N HCl) was added to each vial so that each vial corresponded to a "point" on a titration curve. The samples were equilibrated at 6 °C for 10 days. Then, after in-

† This work was supported by U.S. Public Health Service Grants HL-26335, HL-07291, and HL-07224 and was submitted in partial fulfillment of the requirements for the degree Doctor of Philosophy at Boston University (Cistola, 1985). Preliminary accounts of this work were presented at the Annual Meeting of the American Oil Chemist's Society, Chicago, IL, May 1983, and have been published in abstract form (Cistola et al., 1983).

[1] The term "fatty acids" (when enclosed by quotation marks) refers to the general class of compounds without specification of the ionization state of the carboxyl group. Thus, "fatty acids" could refer to fully un-ionized fatty acids, fully ionized fatty acids (soaps), mixtures of ionized and un-ionized species, and/or 1:1 acid–soap compounds. The term fatty acids (when used *without* quotation marks or qualifying phrases) specifically refers to fully un-ionized (protonated) fatty acids.

[2] Abbreviations: cmc, critical micelle concentration; *F*, number of degrees of freedom; *C*, number of components; *P*, number of phases; SDS, sodium dodecyl sulfate.

0006-2960/88/0427-1881$01.50/0

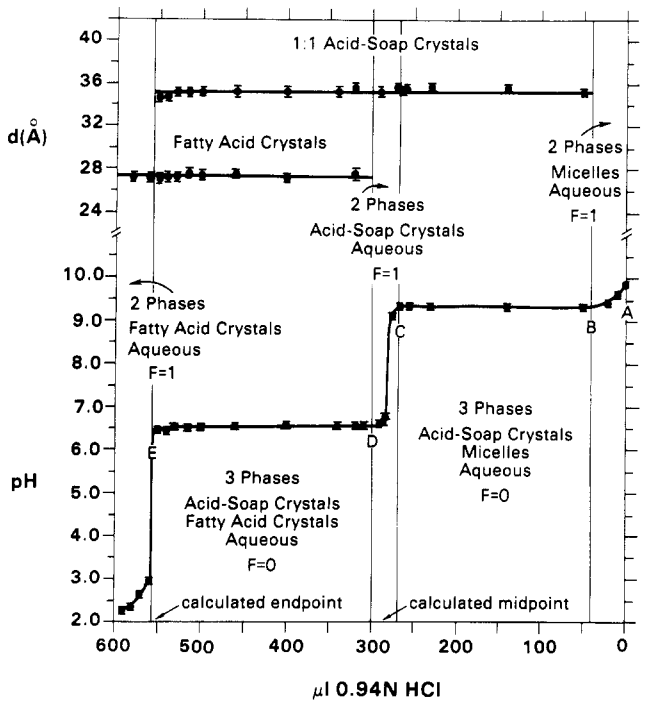

FIGURE 1: Equilibrium titration curve for 0.21 M potassium laurate with added microliters of 0.94 N HCl at 25 °C. The bottom portion of the figure displays pH values, and the top portion displays first-order *d* spacings obtained by X-ray diffraction. The vertical axes (A–E) represent phase boundaries. In the middle of the figure, the number and types of phases present and the number of degrees of freedom (*F*) within each region are noted (see Discussion). Each pH value was obtained from a different individual sample at equilibrium (see Materials and Methods).

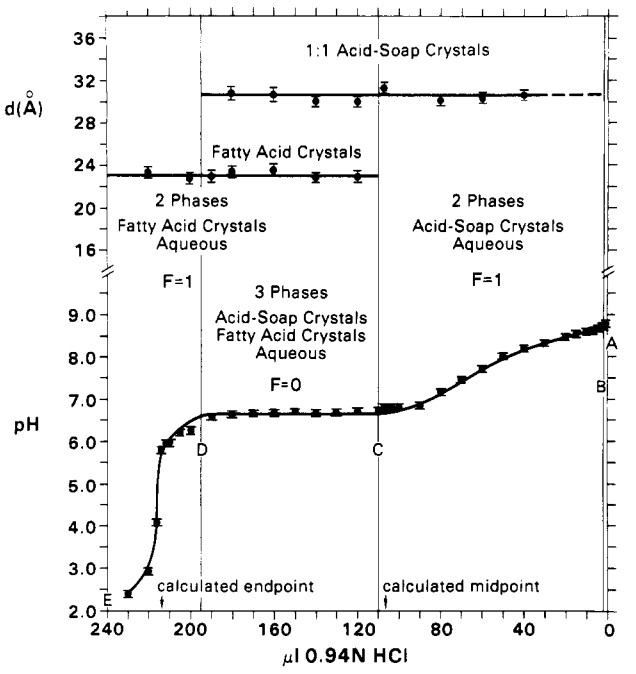

FIGURE 2: Equilibrium titration curve for 0.08 M potassium decanoate with added microliters of 0.94 N HCl at 6 °C. For additional information, see Figure 1 caption.

cubation of the pH meter, electrode, and buffer solutions at 6 °C for 5 h, two separate pH measurements were made on each sample at 6 °C, and the gross visual sample appearance was noted. Following these pH measurements, the same samples were equilibrated at 25 °C for 2 days. pH measurements for each sample were made at this temperature, and gross visual appearance was noted. The same samples were then incubated overnight at 39 or 40 °C in a Dubinoff metabolic shaking incubator (Precision). After incubation of the pH electrode at this temperature for 1 h, sample pH values and gross visual observations were recorded. In addition, natural-abundance ^{13}C NMR spectra were recorded for selected samples at this temperature. Finally, the samples were returned to 6 °C, and after several days incubation, aliquots of selected samples were examined by X-ray diffraction. Proof of equilibrium was established by the following criteria: (i) sample appearance and pH measurements did not change over long periods of time (days to weeks); (ii) the same states were reached whether samples were heated or cooled; (iii) the same states were reached whether protonated fatty acids were titrated with base or potassium salts (soaps) were titrated with acid.

X-ray diffraction patterns were recorded at 6 °C by using the instrumentation and methods described previously (Cistola et al., 1986). ^{13}C NMR spectra were recorded at 50.3 MHz with a Bruker WP-200 instrument as described elsewhere (Hamilton & Small, 1981). Unless noted otherwise, spectral conditions included a sweep width of 10 000 Hz, 16 384 time domain points, and a pulse interval of 0.82 s. External deuteriated chloroform and tetramethylsilane in a capillary insert were used as lock/shim signal and chemical shift reference, respectively. Selected samples were examined by phase-contrast and polarized light microscopy using instrumentation previously described (Cistola et al., 1986). All pH measurements were made with a pH meter (Beckman 3560; Fullerton, CA) equipped with a 29 cm × 4 mm glass combination electrode (Markson MiraMark, Phoenix, AZ).

RESULTS

The equilibrium titration curve for 0.21 M potassium laurate at 25 °C is shown in Figure 1. The concentration was above the cmc (0.02 M; Mukerjee & Mysels, 1970) of potassium laurate and above the monomer solubility of lauric acid (12 μM; Bell, 1973). Furthermore, the temperature was below the melting temperatures of lauric acid (44 °C; Lutton, 1967) and hydrated 1:1 potassium hydrogen dilaurate (34 °C; Cistola et al., 1986) but above the critical micellar temperature of potassium laurate (<0 °C; McBain & Sierichs, 1948).

Between 0 and 39 μL of added HCl (interval AB), the pH decreased from 9.9 to 9.3, and the samples were optically clear. However, between 40 and 267 μL (interval BC), the pH remained constant at 9.3 (Figure 1, bottom), and the samples contained suspended crystals. X-ray diffraction patterns of the samples from interval BC exhibited first-order long spacings (35.3 Å, Figure 1, top) that corresponded to those for crystalline 1:1 potassium hydrogen dilaurate, a 1:1 acid–soap compound (Piper, 1929; Cistola et al., 1986). Between 267 and 300 μL of added HCl (interval CD, a region that included the calculated ionization midpoint), the pH decreased from 9.3 to 6.5. Between 300 and 559 μL (interval DE), the pH remained constant at 6.5, and the samples contained a clear liquid with suspended crystals. X-ray diffraction patterns of samples from interval DE contained two sets of long spacings: one corresponding to 1:1 acid–soap crystals and the other to lauric acid crystals (Figure 1, top). At >559 μL of HCl (beyond point E), the pH dropped from 6.5 to <2.5, and only lauric acid crystals were detected by X-ray diffraction. The experimentally determined ionization end point agreed with the calculated end point (559 μL of HCl).

The equilibrium titration curve for 0.08 M potassium decanoate at 6 °C is shown in Figure 2. The decanoate system was chosen for two reasons. First, unlike the longer chain "fatty acids", decanoate could conveniently be studied above

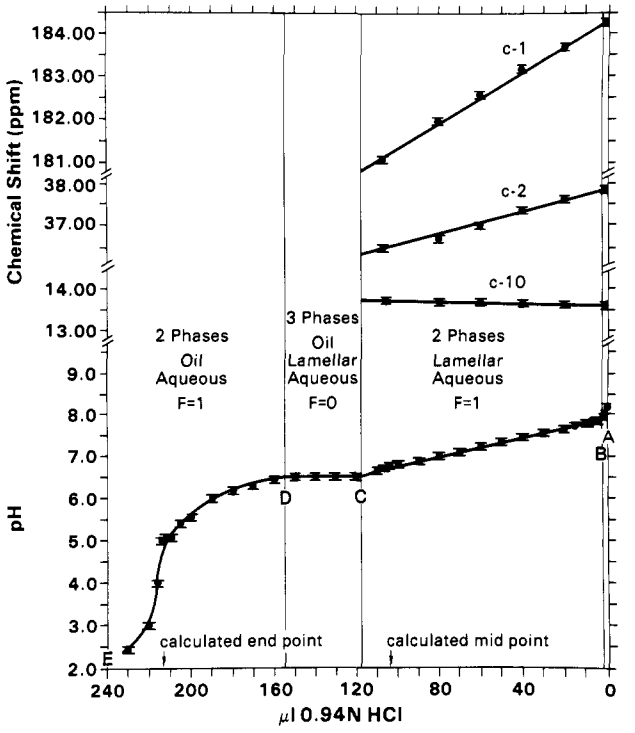

FIGURE 3: Equilibrium titration curve for 0.08 M potassium decanoate at 39 °C. The bottom portion of the figure displays pH values, and the top portion shows ^{13}C NMR chemical shifts of the carboxyl carbon (C-1), α-carbon (C-2), and terminal methyl carbon (C-10) resonances. The vertical axes (A–E) denote phase boundaries. In the middle of the figure, the number and types of phases present and the number of degrees of freedom (F) in each region are noted (see Discussion).

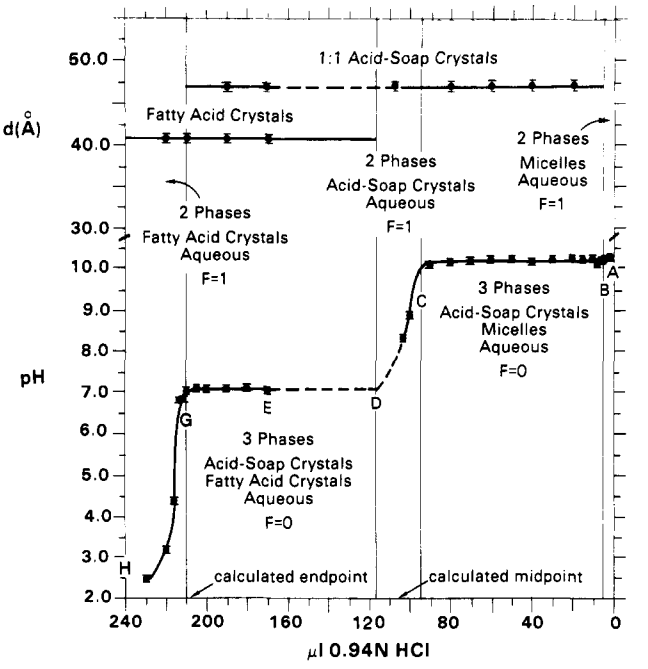

FIGURE 4: Equilibrium titration curve for 0.08 M potassium oleate with added microliters of 0.94 N HCl at 6 °C. The bottom portion of the figure displays pH values, and the top portion shows first-order d spacings obtained by X-ray diffraction. The vertical axes (A–E, G–H) indicate phase boundaries. In the middle of the figure, the number and types of phases and the number of degrees of freedom (F) are noted. The dashed lines indicate expected (interpolated) values over regions that have not been fully characterized under equilibrium conditions (see Results).

and below its cmc and melting temperatures. Second, unlike the shorter chain "fatty acids", decanoate forms stable lamellar fatty acid/soap[3] aggregates near half-ionization (Cistola et al., 1986). In Figure 2, the decanoate concentration (0.08 M) was below the CMC for potassium decanoate (0.1 M; Mukerjee & Mysels, 1970) but above the monomer solubility limit for decanoic acid (0.25 mM; Bell, 1973). The temperature was below the melting temperatures for decanoic acid (32 °C; Lutton, 1967) and hydrated 1:1 potassium hydrogen didecanoate (23 °C; Cistola et al., 1986). The main difference between the laurate system shown in Figure 1 and the decanoate system shown in Figure 2 was that the latter was below the cmc of the potassium soap.

With no added HCl (vertical axis A in Figure 2), the pH was 8.8, and the sample was optically clear. Crystals appeared in the sample with addition of only 2 μL of HCl, and the quantity of the crystals increased with increasing HCl. X-ray diffraction patterns of these samples contained first-order long spacings (Figure 2, top) that corresponded to 1:1 potassium hydrogen didecanoate (Cistola et al., 1986). The pH profile over interval BC (2–107 μL of HCl) was not flat, unlike the analogous region for 0.21 M potassium laurate (Figure 1, interval BC). In interval CD (108–190 μL of HCl), the pH values remained constant at 6.7, and an additional crystalline phase, as distinguished by X-ray diffraction long spacings, appeared in the sample. These long spacings (Figure 2, top) corresponded to first-order reflections for decanoic acid (23 Å; Cistola et al., 1986). In interval DE (>190 μL of HCl), the pH decreased, and only decanoic acid crystals were detected in the sample.

[3] We use the following terminology to distinguish single compounds from mixtures of two compounds. The phrase "1:1 acid–soap" indicates one compound of fixed stoichiometry whereas "fatty acid/soap" indicates a mixture of two compounds with variable stoichiometry.

An equilibrium titration curve for 0.08 M potassium decanoate at 39 °C is shown in Figure 3. In contrast to Figure 2, the temperature (39 °C, Figure 3) was above the melting temperatures for decanoic acid and hydrated 1:1 potassium hydrogen didecanoate (Cistola et al., 1986). With no added HCl (Figure 3, vertical axis A), the samples (pH 8.1) were optically clear, and the ^{13}C NMR carboxyl chemical shift was 184.25 ppm, a value characteristic for aqueous, monomeric, fully ionized fatty acids (Cistola et al., 1982, 1987a). Between 2 and 118 μL (interval BC), the pH decreased from 8.1 to 6.6, and the sample became increasingly turbid and viscous, forming a slightly blue, transluscent gel. The ^{13}C NMR chemical shifts of the C-1 (carboxyl) and C-2 (α-methylene) carbons decreased linearly (Figure 3, top). This linear decrease in chemical shift was similar to that seen for monomeric "fatty acids", but the slope of the line was steeper. The total carboxyl chemical shift change at half-ionization was 3.7 ppm, as compared to 2.5 ppm for monomeric "fatty acids" (Cistola et al., 1982, 1987a). The chemical shift of the terminal methyl carbon (C-10) increased slightly with added HCl, and the line widths of ^{13}C NMR resonances broadened from 1 to <50 Hz over region BC. Microscopic visualization under polarized light showed no detectable birefringence, but under phase optics showed a heterogeneous population of circular (spherical) particles ≤5 μm in diameter. Taken together, the above observations indicated that "fatty acid" aggregation had occurred over interval BC. On the basis of previous studies, these aggregates consisted of a lamellar fatty acid/soap phase (Cistola et al., 1986) in the form of large unilamellar or oligolamellar vesicles (Hargreaves & Deamer, 1978).

Between 118 and 155 μL of HCl (interval CD), an oil phase floated on top of a turbid aqueous phase, and pH values remained constant at 6.5. Above 155 μL (interval DE), a transparent oil phase floated above a transparent aqueous phase, and pH values decreased with added HCl. Because of

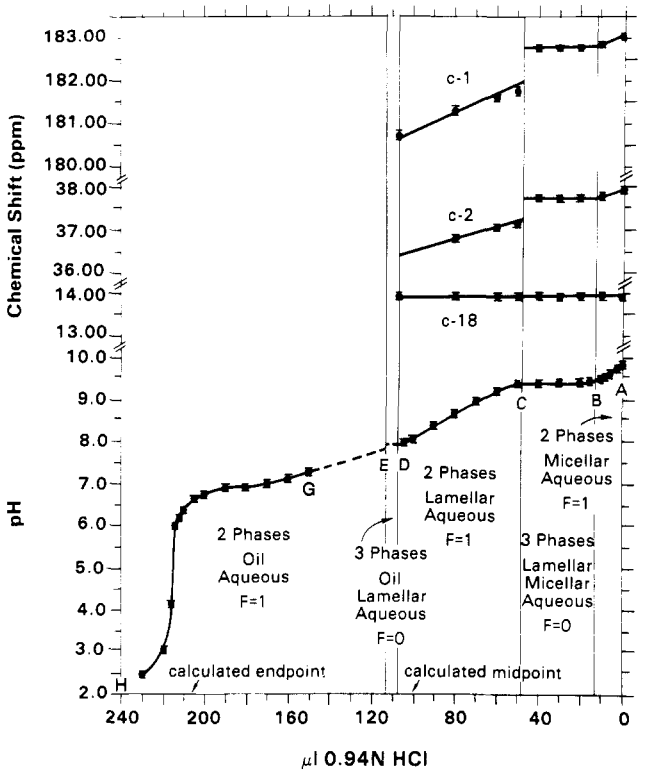

FIGURE 5: Equilibrium titration curve for 0.08 M potassium oleate with added microliters of 0.94 N HCl at 40 °C. The bottom portion of the figure displays pH values, and the top portion shows ^{13}C NMR chemical shift values for the carboxyl carbon (C-1), α-carbon (C-2), and terminal methyl carbon (C-18) resonances. Additional information as in Figure 4 caption.

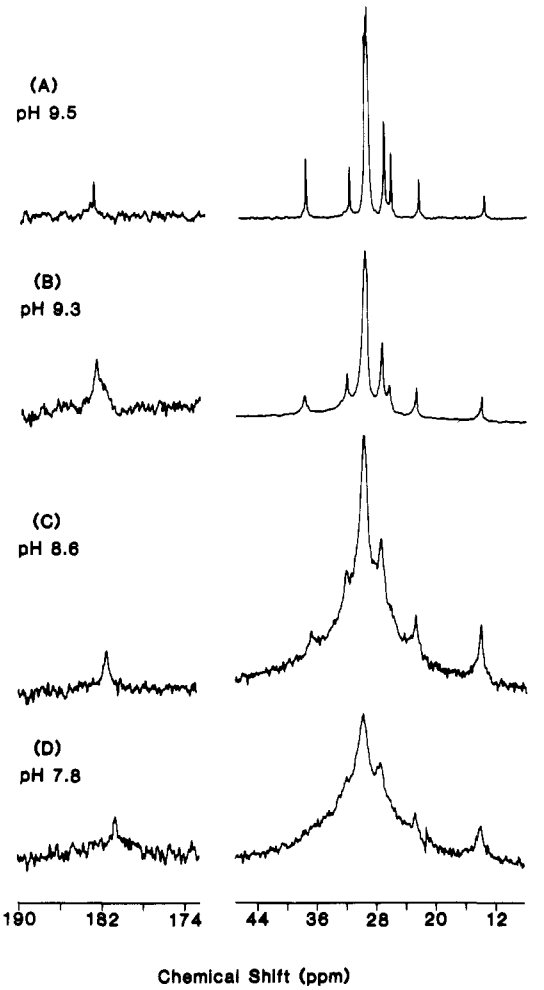

FIGURE 6: Natural-abundance ^{13}C NMR spectra of 0.08 M potassium oleate titrated with varying amounts of 0.94 N HCl at 40 °C. Each spectrum corresponds to a different point on the previous titration curve (Figure 5). (A) Spectrum from interval AB (0 μL of HCl added; Figure 5), 11 044 transients; (B) from interval BC (40 μL of HCl added), 85 006 transients; (C) from interval CD (80 μL of HCl added); (D) from interval DE (108 μL added), 40 875 transients. Different vertical scaling factors were used in spectra A–D, and each spectrum was processed with 5-Hz line broadening. Carboxyl carbon line widths were as follows: (A) 1 Hz; (B) 27 Hz; (C) 25 Hz; (D) 20 Hz.

phase separation, NMR data collection was impractical between vertical axes C and E.

An equilibrium titration curve for 0.08 M potassium oleate at 6 °C is shown in Figure 4. This system was chosen as an example of a biologically relevant long-chain "fatty acid", and because its melting transitions were in a convenient temperature range similar to those for the decanoate system. However, the concentration used (0.08 M) was above the cmc of the potassium soap, whereas 0.08 M potassium decanoate was below its cmc.

Between 0 and 5 μL of HCl (interval AB, Figure 4), the pH decreased from 10.5 to 10.2, and the samples were optically clear. Between 5 and 95 μL of HCl (interval BC), the pH remained constant at 10.2, and the samples contained crystals suspended in a clear liquid. X-ray diffraction patterns of samples from interval BC contained first-order long spacings (Figure 4, top) that corresponded to crystalline 1:1 potassium hydrogen dioleate (47.1 Å; Cistola et al., 1986). Between 95 and 117 μL of HCl (interval CD), the pH decreased from 10.2 to 7.1. However, between 105 and 170 μL of HCl (dashed line), samples contained a white pasty material which disappeared very slowly with time (weeks to months). Because of the uncertainty in whether samples in this range were at equilibrium at the time of pH measurement (after 10 days equilibration), experimental values were omitted from Figure 4, and dashed lines were included to denote the expected equilibrium extrapolation from region EF and comparison with Figure 1. Although the structure of this white pasty material was not established in this study, another laboratory has identified it as a metastable cubic phase (water-in-oil lattice, space group P_n3_m; J. Seddon, personal communication).

Between 170 and 210 μL of HCl (region EG), pH values remained constant at 7.1, and samples contained crystals suspended in a clear liquid. X-ray diffraction patterns of these samples exhibited first-order long spacings (Figure 4, top) characteristic of crystalline 1:1 potassium hydrogen dioleate (47 Å) and crystalline oleic acid (41 Å). Above 210 μL of HCl (region GH), pH values decreased from 7.1 to <2.5, and only crystalline oleic acid was detected by X-ray diffraction.

Equilibrium titration curves for the same system at 40 °C are shown in Figure 5. In this case, the temperature was above the melting transitions for oleic acid (16 °C) and hydrated 1:1 potassium hydrogen dioleate (11 °C; Cistola et al., 1986). Between 0 and 13 μL of HCl (interval AB), the pH decreased from 9.9 to 9.4, and the samples were optically clear. ^{13}C NMR chemical shifts of the carboxyl (C-1) and α-methylene (C-2) carbons (Figure 5, top) decreased over this region. The carboxyl chemical shift at vertical axis A was 183.1 ppm, a value characteristic of micellar aggregates of fully ionized "fatty acids" (D. Cistola, D. Small, and J. Hamilton, unpublished observations), and the NMR lines were narrow (Figure 6A). Between 13 and 48 μL of HCl (interval BC), pH values remained constant at 9.3, and the samples were visibly turbid and translucent. ^{13}C chemical shifts remained constant over interval BC (Figure 5, top), and the NMR lines were broader over interval BC (Figure 6B) than those over

interval AB (Figure 6A). Between 48 and 108 μL of HCl (interval CD), pH values and ^{13}C chemical shifts decreased (except for terminal methyl carbon chemical shift), and NMR peaks broadened further (Figure 6C,D). Polarized light microscopy showed no detectable birefringence, but phase-contrast microscopy of samples from interval CD revealed a heterogeneous population of large liposomes (<5 μm in diameter) similar to those described previously (Hargreaves & Deamer, 1978). The region between 108 and 150 μL (Figure 5, interval DG) remains partially undefined because of excessively long equilibration times (see above). Between 150 and 240 μL of HCl (interval GH), the pH decreased from 7.3 to <2.5, and the samples contained an oil phase floating on a clear liquid.

Discussion

Application of the Gibbs Phase Rule. Equilibrium titration curves have been obtained for "fatty acids" in water above and below cmc values and above and below fatty acid and 1:1 acid–soap melting temperatures. In addition, X-ray diffraction, ^{13}C NMR spectroscopy, phase-contrast and polarized light microscopy, and gross visual observations have been used to characterize the physical states formed by "fatty acids" as a function of ionization state. To aid in the interpretation of these results, the Gibbs phase rule has been applied. The phase rule provides a theoretical framework that (i) explains the shape of a titration curve for a given system, (ii) predicts the number of components or number of phases present in the system, (iii) defines the number of independent variables which need to be fixed in order to completely describe the state of the system, (iv) permits interpolation of physicochemical data to other ionization states, and (v) predicts the composition (ratio of ionized to un-ionized fatty acid) of a given phase present in the system.

For example, consider interval DE in Figure 1. Three phases were present: 1:1 acid–soap crystals and fatty acid crystals (as documented by X-ray diffraction) and an aqueous phase (as documented by visual observation). In addition, there were three components present in the system (potassium laurate, H_2O, and HCl or potassium laurate, lauric acid, and H_2O).[4] Therefore, the phase rule predicted (at constant temperature and pressure) that $F = C - P$ or $F = 3 - 3 = 0$. This condition of invariance ($F = 0$) dictated that the state of the system would be completely fixed over the entire region. Hence, the measured pH value should have been constant over this entire region, a prediction confirmed by our results (Figure 1, region DE).

Invariance was also seen in region BC (Figure 1). There were at least two phases detected (crystalline 1:1 acid–soap and an aqueous phase) in this three-component system. The phase rule ($F = C - P$) predicted $0 = 3 - P$, that is, $P = 3$. Therefore, an undetected third phase must have been present. Since the concentration (0.21 M) was above the cmc (0.1 M) and the temperature was above the critical micellar temperature (<0 °C) for potassium laurate, this third phase must have been micelles. The micellar phase became saturated with protonated fatty acids at point B, corresponding to a composition of 1.0:6.1 un-ionized/ionized species.

In a previous study, Hargreaves and Deamer (1978) presented a titration curve for potassium laurate at 25 °C that was similar to ours (Figure 1). They noted that "the appearance of a plateau (buffering capacity) at a precise pH during titration was coincident with the formation of lipid crystals". These observations are generally consistent with ours, but we propose that the observed plateaus resulted from invariance ($F = 0$) rather than merely from "buffering capacity". This invariance is predicted by the Gibbs phase rule for a system containing three phases and three components at constant temperature and pressure. In addition, the plateaus in the titration curves presented by Hargreaves and Deamer were not completely flat; this suggests that pH measurements were made on sample(s) that had not fully reached equilibrium.

In the decanoate system *below* the cmc of the potassium soap (Figure 2), no plateau was observed below the ionization midpoint (Figure 2, interval AC). Since there was no micellar phase present, the phase rule predicted that $F = 3 - 2 = 1$ and that no plateau would be expected. However, a plateau indicative of invariance was seen in interval CD (Figure 2) since three phases were present in this region.

Micelle Formation and Phase Separation. The issue of whether micelles can be treated as a separate phase has been debated for over a half-century. A number of physical properties (e.g., osmotic pressure, turbidity, equivalent conductance, etc.) exhibit fairly abrupt changes at or near the CMC in solutions that form micelles, and many workers have considered micelle formation to exhibit at least some of the properties of a phase change (Shinoda et al., 1963). Hence, a model known as the "phase-separation" or "two-phase" model has often been used to describe the thermodynamics of micelle formation. Hutchinson et al. (1955) and Shinoda (1963) have described micelles as a "pseudophase" and argued that the aggregation number of most micelles is too small to consider them a true phase.

More recently, Mukerjee (1962, 1967), Elworthy and Mysels (1966), and Tanford (1980) have argued that the phase-separation model for micellar solutions is probably inappropriate. The phase-separation model predicts an abrupt, discontinuous change in properties at a unique concentration (a truly critial cmc), a constant monomer activity above the cmc, and a homogeneous (e.g., monodisperse) micellar phase. In contrast, careful experimental measurements have indicated that somewhat gradual, continuous changes occur near the cmc (Williams et al., 1955; Goddard et al., 1957; Elworthy & Mysels, 1966; Mukerjee, 1967), that monomer activities change above the cmc (Mysels et al., 1963; Elworthy & Mysels, 1966), and that micelles appear to be polydisperse (Mysels & Princen, 1959). Because of the apparent incongruities between experimental data and the phase-separation model, the model has been considered inappropriate or incorrect.

The experimental findings in the present study, interpreted in light of the Gibbs phase rule, indicated that micelles formed by the potassium salts of "fatty acids" in water did indeed constitute a true thermodynamic phase. Comparison of interval BC in Figures 1, 4, and 5 with interval BC in Figures 2 and 3 indicated that thermodynamic invariance occurred when the concentration of the potassium soap exceeded its cmc. Hence, a third phase must have been present above the cmc, and the identity of this third phase was micellar (as confirmed by ^{13}C NMR chemical shift data). Moreover, the micellar

[4] The number of components (C) is defined as the least number of chemically independent species that is required to describe the composition of every phase in the system. In the Gibbs phase rule, it is the *number* of components, rather than the identity of components, that is of importance. Hence, choosing the identity of the components is somewhat arbitrary. In the case of Figure 1, if the components were chosen as potassium laurate, H_2O, and HCl, then lauric acid would not have been a chemically independent species (component). On the other hand, if the components were chosen as potassium laurate, lauric acid, and H_2O, then HCl would not have been a chemically independent species. In either case, the system contained three components.

phases present in interval BC of Figures 1, 4, and 5 must have been homogeneous and essentially monodisperse over the entire interval BC, since the states of these systems were fixed (zero degrees of freedom). In contrast, the systems contained in interval AB of Figures 1, 4, and 5 had one degree of freedom, and the micellar phases were homogeneous and monodisperse *only at a given composition* (*at a given point along the abscissa*). Stated another way, the composition and physical properties of the micellar phase varied across interval AB.

We propose the following explanation to account for the apparent incongruities between the two-phase model and certain experimental data. The two-phase model was derived for a system that contains two components. Hence, above the cmc, the model assumes two components, two phases, and zero degrees of freedom (at constant temperature and pressure). Experimental systems such as pure sodium dodecyl sulfate (SDS) in water or pure potassium soaps in water appear to contain two components, but actually contain three. Because of the well-known phenomenon of hydrolysis (McBain, 1925), the following equilibria will occur. For the generalized colloidal electrolyte KA in water:

$$2H_2O \rightleftharpoons H_3O^+ + OH^- \quad (1)$$

$$KA \rightleftharpoons K^+ + A^- \quad (2)$$

$$A^- + H_3O^+ \rightleftharpoons HA + H_2O \quad (3)$$

$$HA + OH^- \rightleftharpoons A^- + H_2O \quad (4)$$

At equilibrium, a small but significant amount of HA will be present, and its equilibrium concentration will vary with water concentration. Therefore, the system containing pure KA in water above the cmc contains three components, two phases, and one degree of freedom. This degree of freedom (water or KA concentration) must be specified in order to fix the state of the system. As the concentration changes, the composition and physical properties of the micellar phase change, and hence, the true cmc (the cmc at a fixed concentration) changes. Variation of the true cmc with concentration explains why, in systems such as pure SDS in water, experimentally measured physical properties change continuously, rather than discontinuously, as micelles form. In conclusion, it is inappropriate to test the validity of a theoretical two-phase model for micelle formation that assumes zero degrees of freedom above the cmc with experimental data for systems that contain one degree of freedom above the cmc (e.g., pure SDS in water as a function of concentration).

Characterization of the Fatty Acid/Soap Lamellar Phase. In systems above the melting temperatures of hydrated 1:1 acid–soaps, a lamellar fatty acid/soap phase, rather than a crystalline 1:1 acid–soap[3] phase, was present up to and slightly beyond the titration midpoint (Figure 3, interval BD, and Figure 5, interval BE). This lamellar phase exhibited a visible turbidity that increased with added HCl. A similar turbidity at half-ionization was observed for 1:1 fatty acid/soap aggregates in lamellar liquid-crystalline or unilamellar bilayer phases (Cistola et al., 1986). In addition, ^{13}C NMR titration curves (Figures 3 and 5, top) were steeper than similar curves for monomeric "fatty acids". These results were consistent with the formation of a bilayer phase, since, at a given ionization state, carboxyl chemical shifts of "fatty acids" in bilayers are several parts per million lower than values for aqueous monomeric fatty acids. [For example, at half-ionization, the carboxyl chemical shifts of aqueous monomeric "octanoic acid" and "octanoic acid" incorporated into phospholipid vesicles are 181.9 and 178.4 ppm, respectively (Cistola et al., 1987a).] Moreover, phase-contrast microscopy indicated that the lamellar phase consisted of large spherical vesicles.

From the equilibrium titration curve presented in Figure 5, the composition (ratio of un-ionized to ionized fatty acid molecules) of the lamellar phase could be determined. In Figure 5, the lamellar phase did not exist beyond vertical axis E and, according to the phase rule, did not change composition (since $F = 0$) beyond axis D. Therefore, axis D represents the maximum amount of un-ionized oleic acid that could be incorporated into the lamellar phase. The calculated ratio of un-ionized to ionized fatty acids at axis D was 1:0.8. This ratio is essentially the same as that for potassium decanoate (Figure 3, axis C). At the other extreme, vertical axis C (Figure 5) represents the maximum amount of *ionized* oleate that could be incorporated into the lamellar phase, since the lamellar phase did not change composition in interval BC ($F = 0$). The calculated ratio of unionized to ionized molecules at axis C was 1:2.7. Therefore, for oleic acid/potassium oleate, the lamellar phase had stoichiometries that ranged from approximately 1:1 to 1:3 (un-ionized to ionized species). Under conditions where micelles did not form (e.g., 0.08 M potassium decanoate), the lamellar phase incorporated even higher amounts of ionized species (Figure 3, vertical axis B).

From these results, two important conclusions have been drawn. First, the lamellar phase, unlike the crystalline phases of 1:1 acid–soaps, did not contain a single compound with a fixed stoichiometry of fatty acid to soap, but a variable mixture of two compounds (uncharged fatty acids and anionic soaps).[3] This conclusion was also reached from independent results presented elsewhere. Above a certain temperature, crystalline 1:1 acid–soap compounds in water decompose into a lamellar phase mixture of two compounds: protonated fatty acids and potassium soaps (Cistola et al., 1986). Second, the forces that stabilize the lamellar phase must not depend upon an exact 1:1 stoichiometry of un-ionized to ionized species. This conclusion is contrary to the notion that the pH-dependent association of long-chain fatty acids in water is due to "dimerization" and that the "remarkably strong hydrogen bond between a protonated and unprotonated carboxyl group plays an important role in the association" [quoted from Smith and Tanford (1973); see also Gebicki and Hicks (1976)]. If such hydrogen bonds were necessary for stabilization of lamellar aggregates, then it is unlikely that lamellae would be stable at stoichiometries that deviated significantly from 1:1. The lamellar phase is probably an extended aggregate, rather than a series of dimers, stabilized by a balance of forces including hydrocarbon chain–chain interactions and polar group charge repulsion (Cistola et al., 1986).

Physical States of "Fatty Acids" in Water. Figure 7 schematically summarizes the physical states of medium- and long-chain "fatty acids" at different ionization states (or pH values) and temperatures. At temperatures above their hydrocarbon chain melting temperatures in water (denoted T_c), long-chain "fatty acids" in excess water form an oil phase at pH values <7, a lamellar phase (stacked multilayers or large vesicles) between pH 7 and 9, and a micellar phase at pH values >9. At temperatures $< T_c$, "fatty acids" in excess water form fatty acid crystals, 1:1 acid–soap crystals, and (potassium) soap crystals at pH values <7, 7–9, and >9, respectively. T_c values vary with hydrocarbon chain length and degree of saturation as well as "fatty acid" ionization state and counterion (Cistola et al., 1986; Small, 1986).

Biological Applications. Knowledge of the physical states formed by "fatty acids" in water at a given ionization state aids in predicting the physical states formed by nonesterified "fatty acids" during their transport and metabolism in vivo.

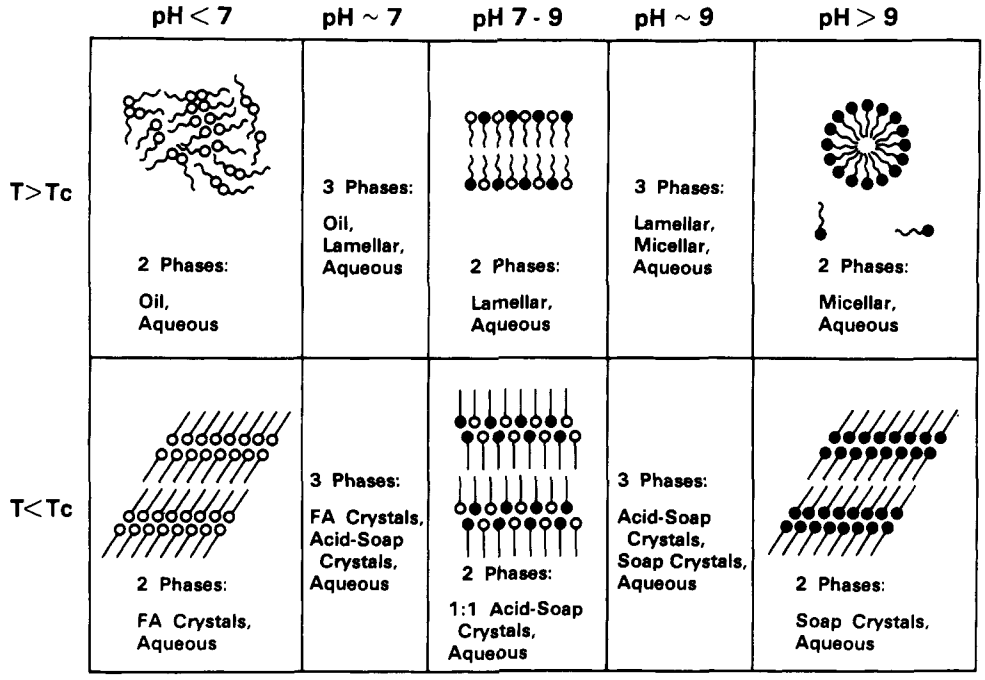

FIGURE 7: Schematic summary of the physical states formed by medium-chain (≥10 carbons) and long-chain fatty acids in excess water as a function of pH and temperature (T). T_c represents the hydrocarbon chain melting temperature in excess water, and T_c differs for fatty acids, 1:1 acid–soaps, and soaps. The aqueous phase is a saturated solution of fatty acid, acid–soap, or soap, and the concentration of these molecules varies with ionization state and hydrocarbon chain length. The closed circles represent ionized (anionic) carboxylate groups and the open circles protonated carboxyl groups. The straight lines represent ordered hydrocarbon chains and the curved lines disordered (liquid) hydrocarbon chains.

In acidic milieu, long-chain fatty acids should be fully protonated and form a stable oil phase (Figure 7). For example, in the stomach lumen, it is likely that fatty acids partition into the oil-phase core of phospholipid/triglyceride emulsion particles (Carey et al., 1983). Fatty acids may also form an oil phase during lipolysis in intracellular lysosomes, since lysosomal pH is low (~4.5). In the cell, cytosolic pH varies between ~6.5 and 7.4, and local accumulations of fatty acids would be expected to form oil and/or lamellar phases (Figure 6). Lamellar structures have been observed by electron microscopy in adipose tissue (Blanchette-Mackie & Scow, 1981) and heart tissue (Wetzel & Scow, 1984) under conditions that cause rapid lipolysis and accumulation of fatty acids. If saturated fatty acids (e.g., "palmitic acid") accumulated preferentially, it is even conceivable that 1:1 acid–soap and/or fatty acid crystals could form within cells.

Nonesterified "fatty acids" are known to have toxic effects on cells under certain conditions (Corr et al., 1984; Spector, 1986). One widely proposed mechanism by which free fatty acids exert cytotoxicity is via so-called "detergent effects" (Pande & Mead, 1968; Katz & Messineo, 1981; Shaw, 1985; Spector, 1986). According to this hypothesis, fatty acids are fully ionized (anionic) at physiological pH, since the apparent pK value for long-chain "fatty acids" in water is thought to be ~4.8 (Goodman, 1958; Spector, 1975). Since fully ionized fatty acids (soaps) form micelles above a critical concentration (cmc), it is proposed that "fatty acid" micelles solubilize membrane lipids and/or proteins and disrupt the physical and functional integrity of cell membranes.

The physicochemical data presented in this paper argue against this hypothesis. First, none of the "fatty acids" in this study formed micelles below pH 9. Rather, at physiological pH, medium- and long-chain fatty acids formed lamellar (bilayer), crystalline, or oil phases. Moreover, we have previously observed that in "fatty acid"/albumin solutions at pH 7.4 and high mole ratios, unbound "fatty acids" form lamellar fatty acid/soap or crystalline 1:1 acid–soap aggregates, but not micelles (Cistola et al., 1987b). Therefore, it seems unlikely that "fatty acids" disrupt cell membranes by micelle formation (detergent solubilization) under physiological or pathological conditions. Second, the experimentally determined pH values at the ionization midpoint (apparent pK_a values) for laurate (pH 8.0; Figure 1), decanoate (pH 6.8; Figures 2 and 3), and oleate (pH 8.0–8.5; Figures 4 and 5) were substantially higher than 4.8. Hence, these "fatty acids" were not fully ionized at physiological pH but were near half-ionization.

Although the pK_a values for *monomeric* "fatty acids" in water are typically 4.8 (Cistola et al., 1982, 1987a), we propose that the higher apparent pK values observed for medium- and long-chain "fatty acids" result from self-association into lamellar or crystalline aggregates. Lamellar fatty acid/soap aggregates have a high negative surface charge density (Cistola et al., 1986), and protons are sequestered at the bilayer surface (an electrical double layer), resulting in a decrease in proton activity (increase in pH) in the bulk solution at a given ionization state (Goddard, 1974). In addition, the local dielectric constant of the medium surrounding the "fatty acid" carboxyl group at the bilayer surface may be lower than that of the bulk aqueous medium; a lowering of the effective dielectric constant would also lead to an elevation of "fatty acid" apparent pK_a values. In systems containing crystalline aggregates (Figures 1, 2, and 4), sequestration of protons by 1:1 acid–soap crystals may result in an increase in pH of the bulk solution.

Under normal conditions in vivo, nonesterified "fatty acids" associate with cellular membranes and binding proteins (Spector, 1986). Fatty acids incorporated into phospholipid bilayer membranes also have elevated apparent pK_a values (pK_a ~ 7.2–7.5), primarily because of the dielectric effect of the nonpolar lipid membrane environment (Ptak et al., 1980; Hamilton & Cistola, 1986). Moreover, it is well established that large amounts (up to 60 mol %) of long-chain "fatty acids" can be incorporated into phospholipid bilayers without disruption of the bilayer structure and that below 60 mol % "fatty

acids" actually stabilize the phospholipid bilayer (Eliasz et al., 1976; Mabrey & Sturtevant, 1977). A similar stabilizing effect has been observed with "fatty acids" incorporated into erythrocyte membranes (Raz & Levine, 1973). The above evidence lends further support to the view that "fatty acids" do not exert detergent effects on cellular membranes in vivo.

We propose that the cytotoxic effects of free fatty acids are more likely mediated by the interaction of "fatty acid" monomers with intrinsic membrane proteins and/or the disruption of proton and calcium gradients. "Fatty acids" have been shown to alter the activity of a variety of enzymes (Pande & Mead, 1968; Spector, 1986; Kelly et al., 1986), to act as proton carriers in phospholipid bilayers (Gutknecht, 1987), and to alter calcium sequestration by the sarcoplasmic reticulum (Watras et al., 1984; Messineo et al., 1984).

Acknowledgments

We thank Dr. David Atkinson for helpful guidance during X-ray diffraction experiments, Donald Gantz for technical assistance with phase-contrast microscopy, and Anne Gibbons for preparation of the manuscript.

References

Bell, G. H. (1973) *Chem. Phys. Lipids 10*, 1–10.

Blanchette-Mackie, E. J., & Scow, R. O. (1981) *J. Ultrastruct. Res. 77*, 295–318.

Carey, M. C., Small, D. M., & Bliss, C. M. (1983) *Annu. Rev. Physiol. 45*, 651–677.

Cistola, D. P. (1985) Ph.D. Dissertation, Boston University, Boston, MA.

Cistola, D. P., Small, D. M., & Hamilton, J. A. (1982) *J. Lipid Res. 23*, 795–799.

Cistola, D. P., Small, D. M., & Hamilton, J. A. (1983) *J. Am. Oil Chem. Soc. 60*, 749.

Cistola, D. P., Atkinson, D., Hamilton, J. A., & Small, D. M. (1986) *Biochemistry 25*, 2804–2812.

Cistola, D. P., Small, D. M., & Hamilton, J. A. (1987a) *J. Biol. Chem. 262*, 10971–10979.

Cistola, D. P., Small, D. M., & Hamilton, J. A. (1987b) *J. Biol. Chem. 262*, 10980–10985.

Corr, P. B., Gross, R. W., & Sobel, B. E. (1984) *Circ. Res. 55*, 135–154.

Eliasz, A. W., Chapman, D., & Ewing, D. F. (1976) *Biochim. Biophys. Acta 448*, 220–230.

Elworthy, P. H., & Mysels, K. J. (1966) *J. Colloid Interface Sci. 21*, 331–347.

Findlay, A. (1951) *The Phase Rule and Its Applications* (Campbell, A. N., & Smith, N. O., Eds.) 9th ed., pp 7–18, Dover Publications, New York.

Fisher, L. R., & Oakenfull, D. G. (1977) *Chem. Soc. Rev. 6*, 25–42.

Gebicki, J. M., & Hicks, M. (1976) *Chem. Phys. Lipids 16*, 142–160.

Goddard, E. D. (1974) *Adv. Colloid Interface Sci. 4*, 45–78.

Goodman, D. S. (1958) *J. Am. Chem. Soc. 80*, 3887–3892.

Gutknecht, J. (1987) *Biochim. Biophys. Acta 898*, 97–108.

Hamilton, J. A., & Small, D. M. (1981) *Proc. Natl. Acad. Sci. U.S.A. 78*, 6878–6882.

Hamilton, J. A., & Cistola, D. P. (1986) *Proc. Natl. Acad. Sci. U.S.A. 83*, 82–86.

Hargreaves, W. R., & Deamer, D. W. (1978) *Biochemistry 17*, 3759–3768.

Katz, A. M., & Messineo, F. C. (1981) *Circ. Res. 48*, 1–16.

Kelly, R. A., O'Hara, D. S., Mitch, W. E., & Smith, T. W. (1986) *J. Biol. Chem. 261*, 11704–11711.

Lutton, E. S. (1967) in *Fatty Acids* (Markley, K. S., Ed.) 2nd ed., Part 4, pp 2586–2592, Interscience, New York.

Mabray, S., & Sturtevant, J. M. (1977) *Biochim. Biophys. Acta 486*, 444–450.

McBain, J. W. (1925) *Nature (London) 115*, 805–807.

McBain, J. W., & Sierichs, W. C. (1948) *J. Am. Oil Chem. Soc. 25*, 221–225.

Messineo, F. C., Rathier, M., Favreau, C., Watras, J., & Takenaka, H. (1984) *J. Biol. Chem. 259*, 1336–1343.

Mukerjee, P. (1962) *J. Phys. Chem. 66*, 1375–1376.

Mukerjee, P. (1967) *Adv. Colloid Interface Sci. 1*, 241–275.

Mukerjee, P., & Mysels, K. J. (1971) *Critical Micelle Concentration of Aqueous Surfactant Systems*, National Bureau of Standards, Washington, DC.

Mysels, K. J., & Princen, L. H. (1959) *J. Phys. Chem. 63*, 1696–1700.

Mysels, K. J., Mukerjee, P., & Abu-Hamdiyyah, M. (1963) *J. Phys. Chem. 67*, 1943.

Pande, S. V., & Mead, J. F. (1968) *J. Biol. Chem. 243*, 6180–6185.

Piper, S. H. (1929) *J. Chem. Soc.*, 234–239.

Ptak, M., Egret-Charlier, M., Sanson, A., & Bouloussa, O. (1980) *Biochim. Biophys. Acta 600*, 387–397.

Raz, A., & Livine, A. (1973) *Biochim. Biophys. Acta 311*, 222–229.

Shaw, W. (1985) *Clin. Chem. (Winston-Salem, N.C.) 31*, 1109–1115.

Small, D. M. (1986) *Lipid Res. 4*, 285.

Smith, R., & Tanford, C. (1973) *Proc. Natl. Acad. Sci. U.S.A. 70*, 289–293.

Spector, A. A. (1975) *J. Lipid Res. 16*, 165–179.

Spector, A. A. (1986) in *Biochemistry and Biology of Plasma Lipoproteins* (Scanu, A. M., & Spector, A. A., Eds.) p 247, Marcel Dekker, New York.

Tanford, C. (1980) *The Hydrophobic Effect: Formation of Micelles and Biological Membranes*, 2nd ed., pp 63–70, Wiley-Interscience, New York.

Watras, J., Messineo, F. C., & Herbette, L. G. (1984) *J. Biol. Chem. 259*, 1319–1324.

Wetzel, M. G., & Scow, R. O. (1984) *Am. J. Physiol. 246*, C467–C485.